RESEARCH PAPER

Facile Preparation and Characterization of SiO_2 Nano-Size Particles: a Study on the Relation Between Contact Angle and Different Processing Parameters

S.M. Alduwaib*, Muhannad M. Abd, Israa Mudher Hassan

* *Salah.aldin@uomustansiriyah.edu.iq*

Department of Science, Collage of basic education, Mustansiriyah University, Baghdad, Iraq

Received: March 2022 **Revised: June 2022** **Accepted: July 2022**

DOI: 10.22068/ijmse.2732

Abstract: *Superhydrophobic materials with contact angle higher than 150°, are very important for researchers. In this research, silica nano-size powders were synthesized using an inexpensive sodium silicate source and a very simple and facile method. Synthesis of hydrophobic solution was carried out by sol-gel method. The surface modification of silica nano-size powders was achieved using different silane/siloxane polymers after which, they were deposited on glass slides. XRD, FESEM, EDX, TEM, FTIR, and Raman analysis were used in the characterization of resulting samples. The XRD results showed a very wide peak around $2\theta = 24.7°$ indicating the amorphous nature of the silica particles. The results also confirmed the synthesis of silica nano-size powder with the size of less than 25 nm. The EDX spectrum showed only the presence of Si and O in the structure and no other elements were visible in the spectreum. The contact angle between water droplet and thin films was measured and the effect of different synthesis parameters on the contact angle was studied. Among the studied polymers and solvents, the most hydrophobicity was obtained using TMCS polymer and xylene solvent. The optimized sample had a maximum contact angle of 150.8°.*

Keywords: *silica nanopowder, silane, siloxane, contact angle, superhydrophobic, sol-gel.*

1. INTRODUCTION

Today, the production of superhydrophobic coatings, considering their widespread applications, are very important for researchers. Superhydrophobic coatings are used for self-cleaning surfaces, solar panels, water-resistant coatings on car glass, anti-fog surfaces, and antifreeze [1-5]. Superhydrophobic materials are those with contact angle higher than 150 degrees [6]. Among hydrophobic compounds, the use of compounds based on silica nanoparticles is more common [7-11]. The challenge which exists using these materials is that the presence of -OH polar groups in these structures causes hydrophilic properties. Therefore, it is necessary for H, which exists in Si-OH groups, to be replaced with Si-R groups to prevent water absorption and create hydrophobic properties [12].

For the production of silica nanopowder, TEOS precursor is usually used, which is expensive [13-17]. There have been reports of the synthesis of silica nanopowder using sodium silicate, which is very inexpensive [18-20]. To remove the sodium ion, present in sodium silicate, the reaction is performed in an acidic [20] or alkaline environment [18].

Superhydrophobic surfaces usually have high surface roughness and low surface energy [21]. Researchers have used various methods to synthesize hydrophobic surfaces such as phase separation [22], chemical etching [23], sol-gel process [24], plasma treatment [25], and laser fabrication [26]. In this study, sodium silicate, which is inexpensive and available, was used as a precursor for the synthesis of silica nanopowder in an acidic environment. The synthesis was carried out by sol-gel method, which can be produced on a large scale. Optimization of effective parameters in surface hydrophobicity was performed completely and comprehensively.

2. EXPERIMENTAL PROCEDURES

2.1. Raw material

Liquid sodium silicate, hydrochloric acid, ethanol, isopropyl, toluene, xylene, n-hexane, Chlorotrimethylsilane (TMCS), Methyl-trimethoxysilane (MTMS), Polydimethylsiloxane (PDMS), and Decamethylcyclopentasiloxane (D5) were purchased from Sigma-Aldrich. All raw materials used are of high purity and were used without further purification.

2.2. Synthesis of Silica Nanopowder

First, 400 ml of liquid sodium silicate was mixed with 80 ml of hydrochloric acid. HCl was

gradually added to sodium silicate and stirred continuously to form a uniform yellow gel. The resulting gel was left for 24 hours. It was then washed several times with hot distilled water and filtered to completely remove the sodium chloride salt produced. The obtained powder was dried in an oven at 50°C for one hour. The final powder was characterized using XRD, FESEM, TEM, EDX, FTIR, and Raman tests.

2.3. Surface Modification of Silica Nanoparticles

0.3 g of the silica nanopowder, produced in the previous step, was mixed with 10 ml of solvent and placed in ultrasonic for 10 minutes to become a gel-like state. 1 ml of silane or siloxane polymers was added to the silica gel and stirred for 30 minutes at 60°C.

2.4. Production of Hydrophobic Thin Films

The solution obtained in the previous step was applied on glass slides using a brush. The layers were then dried at ambient temperature. This step was repeated 5 times to create a more uniform and thicker coating. To evaluate the hydrophobic properties, contact angle test was taken from the final layers.

To optimize the hydrophobic properties of the synthesized thin films, the effect of various parameters (type of polymer, type of solvent, amount of silica nanopowder, amount of polymer and drying temperature of the layers) was studied.

2.5. Characterizations

To investigate the synthesized silica nanopowder, X-ray diffraction (XRD) apparatus with D8 Advance Bruker YT model was utilized using CuKα radiation with wavelength of λ= 1.5418A° at values of 2θ between 5 and 80 degrees. In order to study the size and shape of the grains, TEM images were prepared using Transmission electron microscopy (TEM) apparatus with EM 208S model (100 KV). For studying the morphology and chemical analysis of silica nanopowder, a field emission scanning electron microscope (FESEM) apparatus with MIRA3 TESCAN-XMU model equipped with analysis (EDX) was utilized. Non-conductive materials must be coated with conductive materials before imaging. For this purpose, the synthesized silica nanoparticles were coated with gold and then scanned.

Raman spectroscopy was performed by Confocal Raman Spectroscopy apparatus with Lab Ram HR model, manufactured by Horiba, Japan. The Fourier transform infrared spectrometer (FTIR) with Nicolet AVATAR370 equipment model in the range of 400-4000 cm^{-1} was used to investigate the chemical bonds of the synthesized powder. To evaluate the self-cleaning properties of the samples, the contact angle of water droplets on the thin films was measured using a digital camera with AM-7013MZT model from Dino Lite Company in Taiwan. Water droplets were placed in five different positions for one sample and its mean was considered as the contact angle.

3. RESULTS AND DISCUSSION

3.1. Morphological Characteristics of Silica Nanoparticles

Figure 1 shows the XRD pattern of silica nanoparticles. The XRD spectrum indicates that they, which synthesized by sol-gel method, are amorphous in nature. The XRD spectrum represents a very wide peak specified at 2θ= 24.7° which indicates the amorphous nature of the silica particles. In the XRD pattern illustrated in Figure 1, the wide peak indicates a high percentage of amorphous silica particles [27]. The 2θ value shown in the XRD spectrum results was compared and verified using the standard JCPDS file, and the XRD result obtained is consistent with the JCPDS file (1711-79). Hence, the XRD results confirm that the synthesized material is amorphous silica particles. FESEM was used to study the morphology of SiO_2 nanoparticles synthesized by sol-gel method.

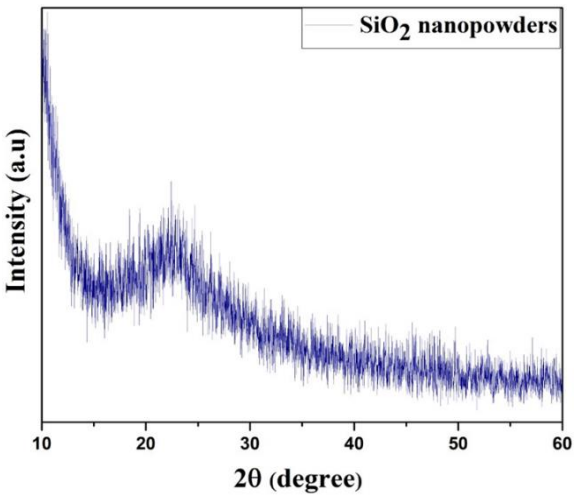

Fig. 1. X-ray diffraction pattern (XRD) of SiO_2 nanoparticles.

The results of the FESEM analysis of surface

morphology on synthesized silica nanoparticles are illustrated in Figure 2 (a). As shown in the figure, the powder contains spherical and completely dense particles. The borders are distributed in the form of discrete structures. The resulting powder is in a network texture with pores. The average physical size of pores is approximately 20-25 nm. Figure 2 (b) shows the EDX spectrum of the synthesized silica nanoparticles. The EDX results confirm the presence of strong signal properties of primary silica.

EDX also indicates the presence of O and Si elements without impurity, which confirm the formation of SiO_2 nanoparticles. Silica nanoparticles show an optical absorption band peak of about 1.8 KeV related to Si element. Sajid and Divasna reported that a strong Si peak occurred at 1.8 KeV, and they also observed O and C elements in the EDX spectrum [28].

Figure 3 shows the FTIR spectrum of silica nanoparticles. According to this spectrum, 760 and 498 cm^{-1} bands are assigned to Si-O-Si tensile and Si-O-Si bending respectively [29]. The absorption bands at 1112 cm^{-1} are because of the siloxane vibrations of the $(SiO)_n$ groups [30]. 3443 and 1634 cm^{-1} peaks are attributed to the O-H tensile bond of the surface of silanol groups and residues of adsorbed water molecules [31].

The Raman spectra of silica nanoparticles are illustrated in Figure 4.

Raman analysis of amorphous silica showed that the spectrum can be characterized in three different areas, a strong polar band at 498 ~ cm^{-1}, then a group of bands of about 795 cm^{-1} with moderate intensity, and some weak bands at 1050 and 1200 cm^{-1}. However, the spectrum was basically dominated by a wide band, which was about 498 cm^{-1} and this was the main area of glass [32]. In this low-frequency area, the band was because of the vibration and bending of the Si-O-Si bond in the SiO_4 tetrahedral. In silica Raman spectrum, two small and sharp bands in 598 cm^{-1} and 690 cm^{-1} were placed on 498 cm^{-1} band.

These two peaks may be attributed to the three- and four-membered silicon and oxygen rings (siloxane rings) in the silica lattice, respectively, or may be due to a structural defect associated with the breaking of Si-O-Si bonds in the silicon lattice (Broken bond model) [33-35]. In fact, the bands in this low-frequency area, that is, the bands located between 400 and 700 cm^{-1}, were all associated with the bond between Si-O-Si tetrahedral.

The bands in the high frequency area near 1050 cm^{-1} and at 1200 cm^{-1} are because of the symmetrical traction of silicon and oxygen on the tetrahedral of silicate with oxygen atoms [32]

Figure 5 shows the TEM micrograph of amorphous silica. TEM analysis also replicates the spherical shape of SiO_2 nanoparticles, and smaller SiO_2 particles cluster to form larger SiO_2s.

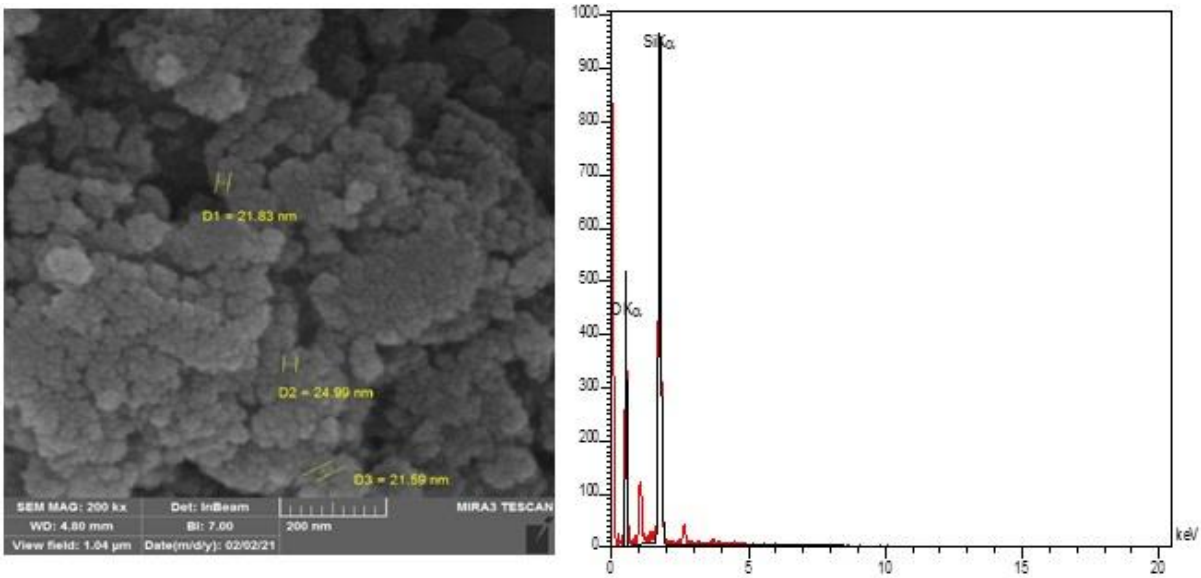

Fig. 2. (a) FESEM images of SiO_2 nanopowder (b) analysis of EDX of SiO_2 nanopowder.

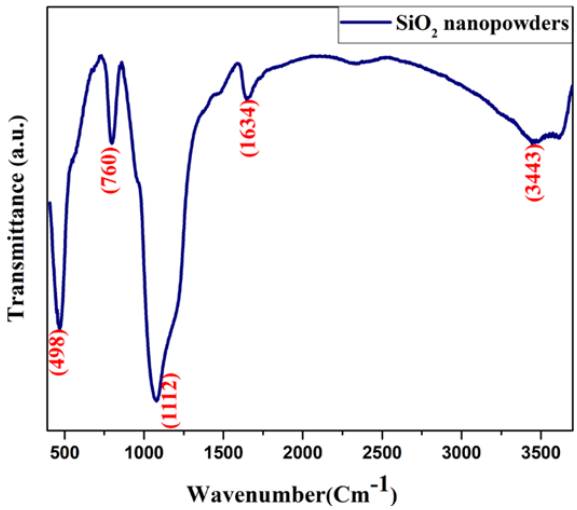

Fig. 3. FT-IR spectra of silica nanoparticle.

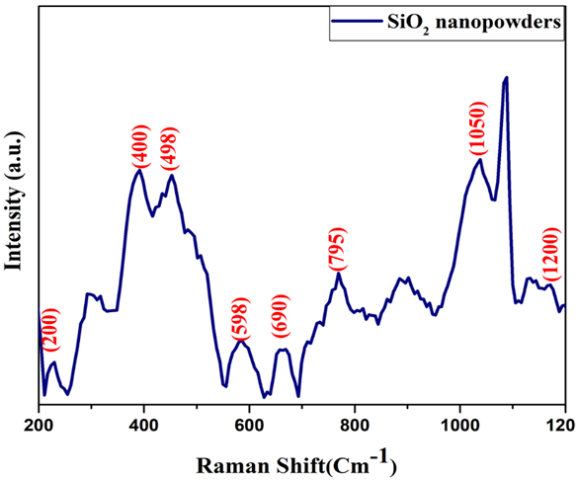

Fig. 4. Raman spectra of amorphous silica nanopowder.

The TEM image also confirms the presence of accumulated SiO_2 nanoparticles.

Apart from the spherical morphology of silica nanoparticles, the cocoon-shaped morphology is also observed in the figure. The shape of cocoon originates from the arrangement of spherical SiO_2 particles together which leads to the accumulation of larger silica particles [36]. The grain size of the nanoparticles, according to the figure below, is 50 nm.

3.2. Investigation of Hydrophobic Properties and Optimization of Parameters

If the contact angle between the three phases of solid, liquid, and gas is less than 90 degrees, the surface is called hydrophilic, which the surface energy of hydrophilic surfaces is very high. While if the contact angle at the point of the contact of liquid drop with solid surface is more than 90 degrees, the surface is called hydrophobic, which hydrophobic surfaces have very low surface energy [6].

To measure the contact angle of the synthesized thin films, an imaging of a 2 µl droplet with a magnification of 50 at 20°C was performed, the results of which are shown in Figures 6 to 11. Figure 6 indicates the effect of using different polymers on the contact angle of the synthesized thin films. The sample is SiO_2 without the use of polymer and its contact angle is 74 degrees. When using MTMS and D5 polymers, the contact angle is reduced and the surface is hydrophilic.

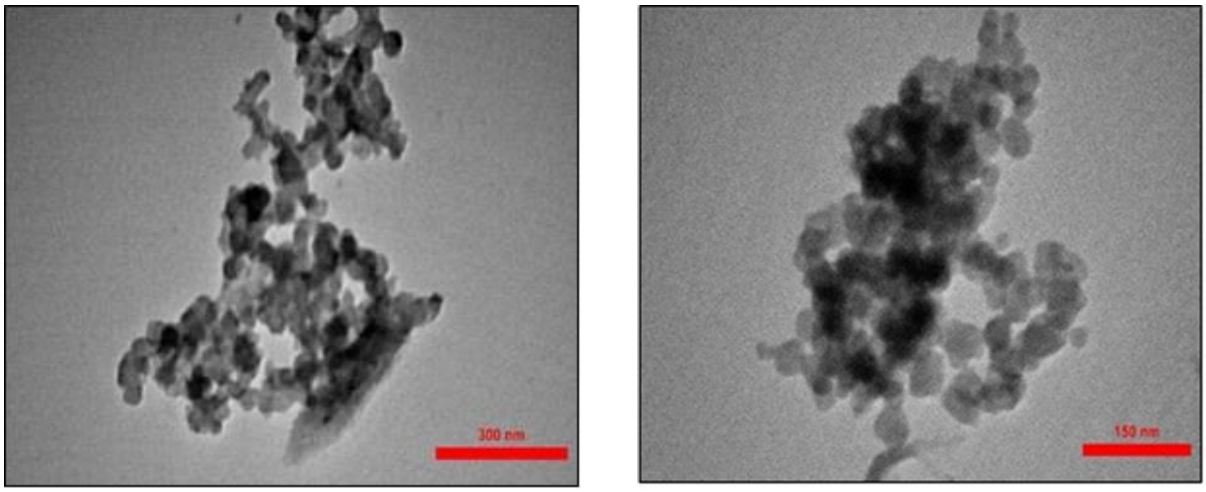

Fig. 5. TEM micrograph of amorphous SiO_2 nanopowder.

However, if PDMS and TMCS polymers are used, the contact angles are 135.5 and 146 degrees, respectively, which indicates the high hydrophobicity of the surface. Therefore, among the studied polymers, the most hydrophobicity was obtained using TMCS polymer, so in the continuation of the optimization steps, TMCS was used to synthesize all samples.

The red rectangles in the Figure 6 show the standard deviation. Since the solution is applied uniformly on the substrate, a slight standard deviation is observed in the results. According to the researcher's results, methyl groups (CH_3) don't increase hydrophobicity, but increase hydrophilicity [37]. By comparing the chemical formula of TMCS, PDMS, MTMS and D5 polymers, it is determined that TMCS has the lowest number of methyl groups and therefore the highest contact angle and the highest hydrophobicity have been obtained using this polymer.

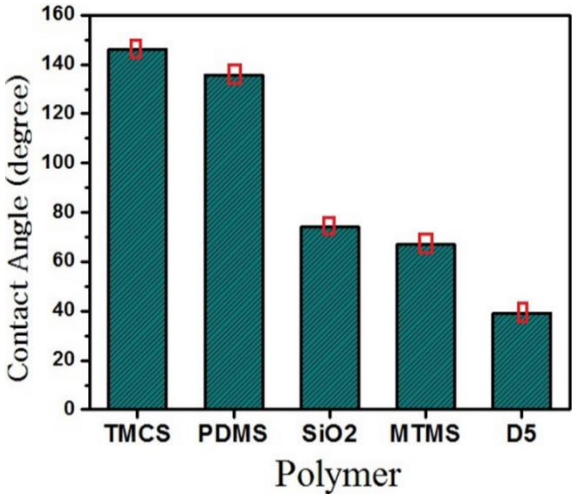

Fig. 6. Comparison of the effect of using different polymers on the contact angle of synthesized thin films. The red rectangles show the standard deviation.

At this stage, the effect of different solvents on the contact angle of the produced thin films was investigated. The studied solvents were n-hexane, ethanol, toluene, isopropyl, and xylene, the results of which are shown in Figure 7. As shown in this Figure, the use of n-hexane solvent caused the surface to become superhydrophilic (contact angle close to zero) and the xylene solvent caused the superhydrophobic surface to be produced at an angle of 146.9 degrees. Therefore, the best solvent for creating hydrophobic properties is xylene so that in the continuation of the sample making process, xylene solvent was used to produce the next samples.

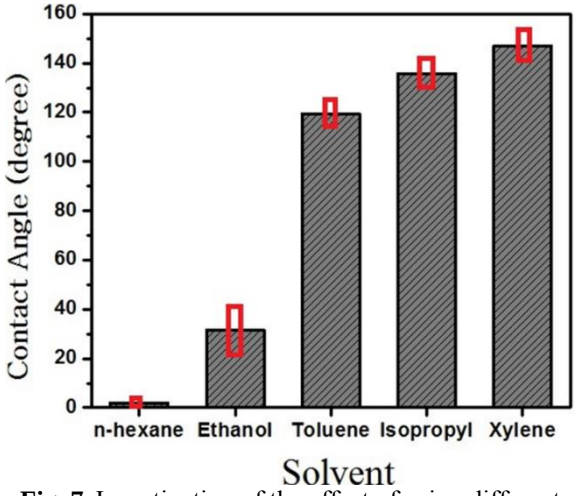

Fig. 7. Investigation of the effect of using different solvents on the contact angle of the produced thin films. The red rectangles show the standard deviation.

Free branches are positively or negatively charged molecules and are therefore hydrophilic because they are adsorbed to polarly charged water molecules [38]. Examining the chemical structure of the solvents used in this study, it is observed that the number of free branches of these solvents that can adsorbed to water for xylene, isopropyl, toluene, ethanol and hexane solvents are equal to 2, 3, 3, 6 and 14 branches. Therefore, xylene, which has the lowest number of free branches, has the most hydrophobic properties, and hexane, which has the highest number of free branches, is completely hydrophilic.

Xylene is illustrated in Figure 8. As shown in the figure, the amount of contact angle increases with the addition of silica from 0.1 to 0.3, and the amount of contact angle decreases with increasing nanoparticles from 0.3 to 0.4. Therefore, the use of 0.3 g of silica caused the maximum amount of contact angle. Silica nanoparticles without surface modification are hydrophilic. By adding various polymers and modifying the surface, SiO_2 nanoparticles show hydrophobic properties. As described in the experimental section, 1 ml of TMCS polymer was added to the silica gel, which seems to be sufficient to modifying the surface of 0.3 g of silica.

By increasing the amount of silica to 0.35 and 0.4 g, some silica nanoparticles remains in the solution which has not been modified and therefore are hydrophilic. Therefore, this causes

the reduction of the contact angle by increasing the amount of silica to more than 0.3 g. In the continuation of the parameter's optimization, 0.3 g of silica was used in the synthesis process.

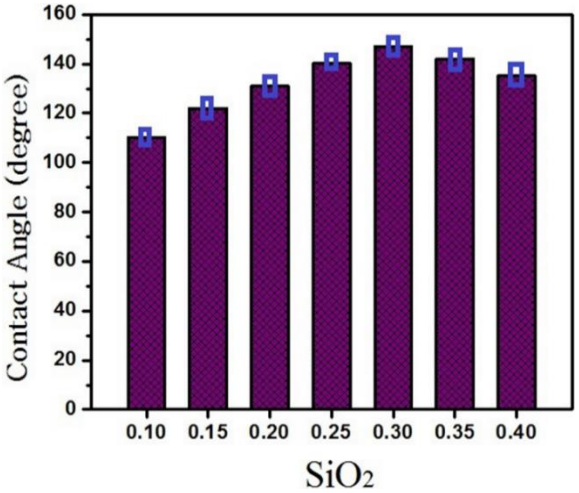

Fig. 8. Investigation and comparison of the contact angle between water droplet and TMCS-modified silica thin films dissolved with xylene with different amounts of silica nanopowder. The blue rectangles show the standard deviation.

In the fourth step, the amount of TMCS polymer was optimized. TMCS was selected as 0.5, 1, 1.5, and 2 ml. The results of contact angle measurements are shown in Figure 9. The best result was obtained using 2 ml of TMCS, where the contact angle between the water droplet and the thin film is 150.2 degrees, which indicates the production of a superhydrophobic surface. In the next step, 2 ml of TMCS was used to synthesize thin films.

In the final step, 0.3 g of silica, 2 ml of TMCS, and xylene solvent were used to synthesize the thin films. After synthesizing the hydrophobic solution and applying it on glass slides, the synthesized layers were placed at different temperatures namely 20, 60, 100, 140, 180, and 220°C.

The effect of temperature on the contact angle of the synthesized thin films was studied and the result is reported in Figure 10. According to this Figure, all samples have a contact angle higher than 140 degrees and the difference between the samples is very small. As the temperature increases, the value of the contact angle decreases.

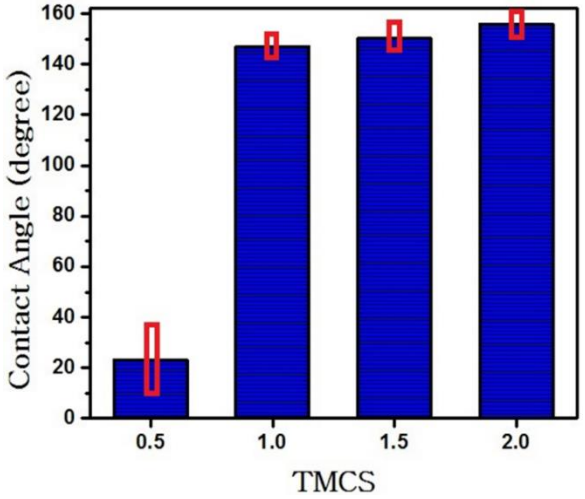

Fig. 9. Investigation and comparison of the contact angle between water droplet and TMCS-modified silica thin films in the presence of different TMCS amounts. The red rectangles show the standard deviation.

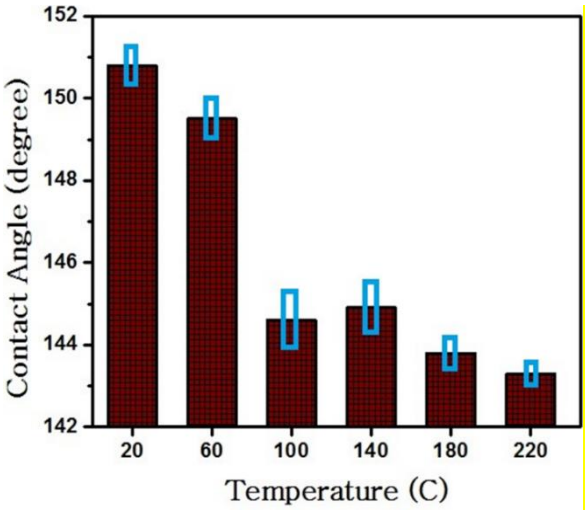

Fig. 10. Investigation of the effect of temperature on the contact angle of synthesized thin films. The blue rectangles show the standard deviation.

As the temperature increases, the hydrophobic interactions changes and the hydrophobicity decreases. Similar results have been reported by researchers [39]. The sample synthesized at ambient temperature (20°C) has a maximum contact angle of 150.8 degrees. The image of the water droplet on the TMCS-modified silica thin film at ambient temperature is shown in Figure 11.

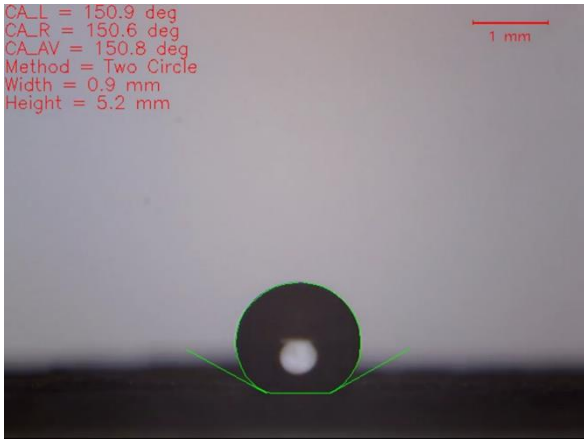

Fig. 11. Contact angle between water droplet and TMCS-modified silica thin film.

4. CONCLUSIONS

Silica nano-meter size powders were synthesized using an inexpensive source of sodium silicate in an acidic environment. Characterization of silica nano-meter size powders was performed using XRD, FESEM, EDX, TEM, FTIR, and Raman spectroscopy. The XRD results confirmed the amorphous nature of the synthesized material. TEM and FESEM results confirmed the synthesis of silica nano-size powders with an average size of less than 25 nm. The synthesis of hydrophobic solution was performed by a very simple sol-gel method. The surface of silica nano-meter size powders were modified using different polymers (PDMS, TMCS, MTMS, D5) before being deposited on glass slides. The contact angle between the water droplet and the synthesized thin films was measured and the effect of different synthesis parameters on the contact angle was studied. The results of parameter optimization demonstrated that the maximum contact angle is obtained using TMCS polymer, xylene solvent, and ambient temperature. The optimum amount of silica nano-size powders were 0.3 g and this amount for TMCS polymer is 2 ml. In general, synthesized thin films had superhydrophobic properties and the method used in this research can be developed for use in an industrial scale.

REFERENCES

[1] Zhou, X, Yu, S.R, Jiao, S.Z, Lv, Z.X, Liu, E.Y, Zhao, Y. Cao, N, "Fabrication of superhydrophobic TiO_2 quadrangular nanorod film with self-cleaning, anti-icing properties" J. Ceram. Int., 2019, 45, 11508-11516.

[2] Zhao, R, Chen, Y, Liu, G.Z, Jiang, Y.C, Chen, K.L, "Fabrication of self-healing water based superhydrophobic coatings from POSS modified silica nanoparticles." J. Mater. Lett., 2018, 229, 281-285.

[3] Feng, L.B, Yan, Z.N, Shi, X.T, Sultonzoda, F, "Anti-icing/frosting and self-cleaning performance of superhydrophobic aluminum alloys." J. Appl. Phys. A, 2018, 124 142.

[4] 4. Mahadik, S.A, Parale, V, Vhatkar, R.S, Mahadik, D.B, Kavale, M.S, Wagh, P.B, Gupta, S. Gurav, J, "Superhydrophobic silica coating by dip coating method." J. Appl. Surf. Sci, 2013, 277, 67-72.

[5] Vengatesh, P, Kulandainathan, M.A, "Hierarchically ordered self-lubricating superhydrophobic anodized aluminum surfaces with enhanced corrosion resistance." J. ACS Appl. Mater. Interfaces, 2015, 7, 1516-1526.

[6] Liao, R.J, Zuo, Z.P, Guo, C. Yuan, Y. Zhuang, A.Y. "Fabrication of superhydrophobic surface on aluminum by continuous chemical etching and its anti-icing property." J. Appl. Surf. Sci, 2014, 317, 701-709.

[7] Cabañas, A. Enciso, Carmen Carbajo, E. M, Torralvo, M.J. Pando, C. Renuncio, J.A.R. "Studies on the porosity of SiO_2-aerogel inverse opals synthesised in supercritical CO_2." J. Micropor. Mesopor. Mater, 2007, 99, 23–29.

[8] He, F, Zhao, H, Qu, X, Zhang, C, Qiu, W, "Modified aging process for silica aerogel." J. Mater. Process. Technol, 2009, 209, 1621–1626.

[9] Mahadik, D.B. Rao, A.V. Kumar, R. Ingale, S.V. Wagh, P.B. Gupta, S.C. "Reduction of processing time by mechanical shaking of the ambient pressure dried TEOS based silica aerogel granules." J. Porous Mater, 2012, 19, 87–94.

[10] Omranpour, H, Motahari, S, "Effects of processing conditions on silica aerogel during aging: role of solvent, time and temperature." J. Non-Cryst. Solids, 2013, 379 7–11.

[11] Mahadik, S.A, Kavale, M.S, Mukherjee, S.K, Rao, A.V, "Transparent

Superhydrophobic silica coatings on glass by sol–gel method." J. Appl. Surf. Sci, 2010, 257, 333-339.

[12] Yokogawa, H, Yokoyama, M, Takahama K, and Uegaki, Y, "Preparation and characterization of superhydrophobic glass surface using pyrophyllite nanosilica coating." AIP Conference Proceedings, 2016, 1712, 050016.

[13] Shi, F, Niu, J, Liu, J, Liu, F, Wang, Z. Feng, X. Q, Zhang, X, "Towards understanding why a superhydrophobic coating is needed by water striders", J. Adv. Mater, 2007, 19, 2257–2261.

[14] Li, W, Amirfazli, A, "Microtextured superhydrophobic surfaces: a thermodynamic analysis." J. Adv. Colloid Interface Sci, 2007, 132, 51–68.

[15] Li, W, Amirfazli, A, "Hierarchical structures for natural superhydrophobic surfaces." J. Soft Matter, 2008, 4, 462–466.

[16] Li, W. Amirfazli, A, "A thermodynamic approach for determining the contact angle hysteresis for superhydrophobic surfaces." J. Colloid Interface Sci, 2005, 292, 195–201.

[17] Manca, M, Cannavale, A, Marco, L.D, Aricò, A.S. Cingolani, R, Gigli, G, "Durable superhydrophobic and antireflective surfaces by trimethylsilanized silica nanoparticles-based sol–gel processing." J. Langmuir, 2009, 25, 6357–6362.

[18] Schwertfeger F, Frank, D, and Schmidt, M "Hydrophobic water glass-based aerogels without solvent exchange or supercritical drying." J. Non-Cryst. Solids, 1998, 225, 24-29.

[19] Schmidt, M, and Schwertfeger, F, "Applications for Silica Aerogel Products." J. Non-Cryst. Solids, 1998, 225, 364-368.

[20] Uzma, K. H, Bangi, A, Venkateswara, Rao, and Parvathy Rao, A, "A new route for preparation of sodium-silicate-based hydrophobic silica aerogels via ambient-pressure drying." J. Sci. Technol. Adv. Mater, 2008, 9, 035006-035010.

[21] Jiang, L. Wang, R. Yang, B. Li, T.J. Tryk, D.A. Fujishima, Hashimoto, A. K. Zhu, D.B, "Binary cooperative complementary nanoscale interfacial materials." J. Appl. Chem, 2000, 72, 73-81.

[22] Hejazi, I, Hajalizadeh, B, Seyfi, J, Sadeghi, G.M.M, Jafari, S.-H. Khonakdar, H.A, "Role of nanoparticles in phase separation and final morphology of superhydrophobic polypropylene/zinc oxide nanocomposite surfaces." J. Appl. Surf. Sci, 2014, 293, 116-123.

[23] Liao, R.J, Zuo, Z.P, Guo, C, Yuan, Y, Zhuang, A.Y, "Fabrication of superhydrophobic surface on aluminum by continuous chemical etching and its anti-icing property." J. Appl. Surf. Sci, 2014, 317, 701-709.

[24] Mahadik, S.A. Kavale, M.S. Mukherjee, S.K. Rao, A.V, "Transparent Superhydrophobic silica coatings on glass by sol–gel method." J. Appl. Surf. Sci, 2010, 257, 333-339.

[25] Ryu, J, Kim, K, Park, J.Y, and et all "Nearly perfect durable superhydrophobic surfaces fabricated by a simple one-step plasma treatment." J. Sci. Rep, 2017, 7 1981-1986.

[26] Ta, D.V, Dunn, A, Wasley, T.J, Kay, R.W, and et all, "Nanosecond laser textured superhydrophobic metallic surfaces and their chemical sensing applications." J. Appl. Surf. Sci, 2015, 357, 248-254.

[27] Singho, N. D, and Johan, M. R, "Complex impedance spectroscopy study of silica nanoparticles via sol-gel method," J. International Journal of Electrochemical Science, 2012, 7, 50604- 5615.

[28] Sajid, P. A. R, and Devasena, T, "Synthesis and characterization of silica nanocomposites for bone applications." J. International Research Journal of Pharmaceutical, 2012, 3, 173–177.

[29] Lu, Y, and Yan, X, "An imprinted organic-inorganic hybrid sorbent for selective separation of cadmium from aqueous solution." J. Analytical Chemistry, 2004, 76, 453–457.

[30] Bois, L, Bonhomme, A, Ribes, A, et al. "Functionalized silica for heavy metal ions adsorption." J. Colloids and Surfaces, 2003, 221, 221–230.

[31] Silva, A, Sousa, K, Germano, A, et al. "A new organofunctionalized silica containing thioglycolic acid incorporated for divalent cations removal – A thermodyamic

cation/basic center interaction." J. Colloids and Surfaces, 2009, 332, 144–149.
[32] McMillan, P, "Structural studies of silicate glasses and melts- applications and limitations of Raman spectroscopy." J. Am. Mineral, 1984, 69, 622–644.
[33] Mikkelsen, J.C, Galeener, F.L, "Thermal equilibration of Raman active defects in vitreous silica." J. Non-Cryst. Solids, 1980, 37, 71–84.
[34] Stolen, R.H, Walrafen, G.E, "Water and its relation to broken bond defects in fused silica." J. Chem. Phys, 1976, 64, 2623–2631.
[35] Stolen, R.H, Krause, J.T, Kurkjian, C.R, "Raman scattering and far infrared absorption in neutron compacted silica." J. Discuss. Faraday Soc, 1970, 50, 103–107.
[36] Tadano, T, Zhu, R, Muroga, Y, Hoshi, T, Sasaki, D, Yano, S, Sawaguchi, T, "A new mechanism for the silica nanoparticle dispersion–agglomeration transition in a poly (methyl methacrylate)/silica hybrid suspension." J. Polym, 2014, 46, 342-348.
[37] Koga, Y, Westh, P, Nishikawa, K, Subramanian, S, "Is a Methyl Group Always Hydrophobic? Hydrophilicity of Trimethylamine-*N*-oxide, Tetramethyl Urea and Tetramethylammonium Ion." J. Phys. Chem. B, 2011, 115, 2995–3002.
[38] Senem, A, Kayaa, T, Cengiz, U, "Fabrication and application of superhydrophilic antifog surface by sol-gel method", Progress in Organic Coatings, 2019, 126, 75–82.
[39] Baldwin, R, L, "Temperature dependence of the hydrophobic interaction in protein folding." Proc. Natl. Acad. Sci., 1986, 83, 8069-8072.